Journal of Power Sources 218 (2012) 212–220

Contents lists available at SciVerse ScienceDirect

Journal of Power Sources

journal homepage: www.elsevier.com/locate/jpowsour

Model order reduction for solid-phase diffusion in physics-based lithium ion cell models

Xiao Hu [a,*], Scott Stanton [a], Long Cai [b], Ralph E. White [b]

[a] ANSYS Inc., Canonsburg, PA 15317, USA
[b] Department of Chemical Engineering, University of South Carolina, Columbia, SC 29208, USA

HIGHLIGHTS

- A reduced order model is proposed for solid-phase diffusion.
- The reduced order model is faster than solving the full model and is very accurate.
- Impact of weight function on solution is investigated.
- Step response method is proposed for low frequencies.
- Complex exponential method is proposed for high frequencies.

ARTICLE INFO

Article history:
Received 23 May 2012
Received in revised form
29 June 2012
Accepted 1 July 2012
Available online 7 July 2012

Keywords:
Model order reduction
Lithium ion battery
State space model
LTI systems
Vector fitting

ABSTRACT

A model order reduction method is developed and applied to the solid-phase diffusion problem used in physics-based lithium ion cell models. The reduced order model is in the form of a state space model. Model identification is performed in the frequency-domain using the vector fitting method. The method allows the user to control the order of the model, the frequency band for model identification, and optionally a weight function to give a certain frequency band more weight. The model can be used for spherical and non-spherical particles. For spherical particles, the results from using the reduced order model are compared with those from analytical solutions, and excellent agreement is achieved using 3rd and 5th order models. When the approach is applied to non-spherical particles, the transfer functions need to be calculated numerically. Two methods, step response and complex exponential, are proposed to calculate the required transfer function. While the step response method is more suitable for low frequencies, the exponential method is more accurate for high frequencies.

1. Introduction

The lithium ion battery is a preferred candidate as a power source for hybrid electric vehicles and electric vehicles due to its outstanding characteristics such as high energy density, high voltage, low self-discharge rate, and good stability among others. Physics-based lithium ion battery models are widely used to predict the electrochemical behavior of lithium ion batteries [1–3]. The implementation of such a model requires solving a diffusion problem in the porous electrodes. The diffusion process in the electrodes is by nature 3D because of the rather convoluted shape of the porous structures. Therefore, it is computationally expensive to solve the physics-based lithium ion battery models when 3D diffusion equations are used to characterize the diffusion process. Due to this difficulty, the porous structure is assumed to consist of disconnected spherical particles so that the diffusion equation can be assumed to be one-dimensional. In such an approach, each particle is exposed to different boundary conditions, and therefore the diffusion equation has to be solved for each particle. Due to the large number of particles involved, it is still computationally expensive to solve the physics-based lithium ion battery models when a large number of 1D diffusion equations are solved numerically.

Under the assumption of spherical particles, several methods have been proposed to reduce the size of the problem. They belong to time-domain approach or frequency-domain approach. One time-domain approach makes the assumption that the concentration within each spherical particle can be approximated with a parabolic profile [4,5]. Another time-domain approach obtains an approximate solution by truncating the analytical solution of an infinite series and then adding an estimate term for the truncation

* Corresponding author. Tel.: +1 734 213 1261; fax: +1 734 213 0147.
E-mail address: xiao.hu@ansys.com (X. Hu).

0378-7753/$ – see front matter © 2012 Elsevier B.V. All rights reserved.
http://dx.doi.org/10.1016/j.jpowsour.2012.07.007

error [6]. In these two methods, spherical particles are assumed, and the methods cannot be extended to non-spherical particles. Time-domain methods also cannot control frequency performance easily, while frequency-domain methods can achieve this readily. In frequency-domain approximation methods, a state space model is created to approximate the transfer function of the system. In Ref. [7], high-order poles of the transfer function are truncated and the lower-order poles are grouped together and approximated using a state space model. The proposed 5th order reduced model gives an error of 6.3%. More accurate results can be obtained using the method discussed in this paper. In Ref. [8], a discrete-time state space model is derived from a known transfer function. And then it is converted into a continuous-time state space model. Using the method in this paper, a continuous-time state space model can be generated directly. In both Refs. [7,8], analytical transfer functions are assumed to be known, and thus both methods are limited to spherical particles. The method discussed in this paper can be extended to particles of any shape.

In Ref. [9], Hu et al. proposed a continuous-time state space model, which is created directly from a numerically calculated transfer function. The model is demonstrated to be applicable to particles of any shape. In this paper, the method used in Ref. [9] is improved and refined. It was found that the step response method used in Ref. [9] to calculate the transfer function is very accurate only for relatively low frequencies. This is because magnitudes of high frequency components are much smaller than those of lower frequency components and therefore the step response method gives large numerical error for high frequency components. In this paper, a complex exponential method is proposed to calculate the transfer function for high frequencies. It will be shown in this paper that the complex exponential method gives highly accurate results for high frequencies. But this method is hard to converge for lower frequencies. When the complex exponential method is used together with the step response method, accurate transfer function can be obtained for the entire interested frequency range. Model identification, after the transfer function is determined, is done in the frequency-domain using the vector fitting (VF) method [10]. The VF method is a widely used method for model identification [11–16], and it is the method used in Ref. [9]. In this paper, a weight function is added during the fitting process and its impact on the model performance is investigated.

2. Model development when analytical transfer functions are available

In using the frequency-domain approach, the problem is treated like a system. A system is an entity that processes a set of input signals (or simply called inputs) and yields another set of output signals (or simply called outputs). In such a system view, only the input/output relationship of the system is of interest to the user and the inner structure of the system is not important. In the solid-phase diffusion problem, the molar flux at the particle surface as a function of time is used as the input and the difference between the surface concentration and the average concentration at the particle surface as a function of time is used as the output. We are interested in the relationship between the surface molar flux and the difference between the surface concentration and the average concentration. Concentration distribution inside a particle is not of great interest. Solid-phase diffusion problem, as described above, is a system. More importantly, it is not only a system, but it is also a linear and time-invariant (LTI) system. Any state space model is also an LTI system. One important feature about LTI systems is that if two LTI systems have the same transfer function, the two systems behave identically in that the outputs of the two systems are the same provided that the inputs to the two systems are the same. This feature allows us to use the state space model to simulate the solid-phase diffusion problem provided that its transfer function is curve-fitted to that of the solid-phase diffusion problem. Since the size of the state space model is small, it runs very fast compared with a full model which solves the complete diffusion equation directly using numerical methods.

To demonstrate the state space approach, we first model a spherical particle, for which an analytical transfer function is available. The diffusion of lithium ions in a spherical particle follows the Fick's law and is described by the following partial differential equations:

$$\frac{\partial c}{\partial t} = D\frac{1}{r^2}\frac{\partial}{\partial r}\left(r^2\frac{\partial c}{\partial r}\right) \tag{1}$$

$$c(r, t = 0) = 0 \tag{2}$$

$$\left.\frac{\partial c}{\partial r}\right|_{r=0} = 0 \tag{3}$$

$$-D\left.\frac{\partial c}{\partial r}\right|_{r=R} = j(t) \tag{4}$$

where c is the concentration of lithium in the solid particle; D is the solid-phase diffusion coefficient for lithium in the particle, assumed to be constant; $j(t)$ is the boundary molar flux, assumed to be a function of time; r is the radial coordinate; R is the radius of the spherical particle. Note that we specified the initial condition to be zero in Eq. (2) because such an initial condition is convenient for Laplace transform. The real initial value can simply be added back to the final solution. We are interested in the relationship between $j(t)$ and surface concentration, $c_s = c(R, t)$. From Eqs. (1)–(4), Jacobsen and West [17] found the transfer function:

$$\frac{C_s(s)}{J(s)} = \frac{R}{D}\left[\frac{\tanh(\beta)}{\tanh(\beta) - \beta}\right] \tag{5}$$

with $\beta = R\sqrt{s/D}$. We define the difference between the surface concentration and the average concentration by subtracting the average response $C_{ave}(s) = -3J(s)/(Rs)$ from the surface concentration. $C_{ave}(s)$ is obtained by taking the Laplace transform of the mass conservation equation, $(4/3)\pi R^3(\mathrm{d}c_{ave}(t)/\mathrm{d}t) = j(t)\cdot 4\pi R^2$. Define $\Delta C_s(s) = C_s(s) - C_{ave}(s)$, and the transfer function relating $\Delta C_s(s)$ to $J(s)$ becomes the following:

$$H(s) = \frac{\Delta C_s(s)}{J(s)} = \frac{R}{D}\left[\frac{\left(\beta^2 + 3\right)\tanh(\beta) - 3\beta}{\beta^2(\tanh(\beta) - \beta)}\right] \tag{6}$$

An analytical solution of Eqs. (1)–(4) under a unit step input in non-dimensional form is shown to be an infinite series in Ref. [6]. After converting it into dimensional form, the surface concentration relative to the average concentration under a unit step input of 1 mol m^{-2} s^{-1} is the following,

$$\Delta c_{s,step}(t) = \sum_{n=1}^{\infty} Q_n(t) \quad (t \geq 0) \tag{7}$$

where

$$Q_n(t) = -\frac{R}{D}\frac{2}{\lambda_n^2}\left[1 - \exp\left(-\lambda_n^2\frac{D}{R^2}t\right)\right] \tag{8}$$

$$\lambda_n - \tan(\lambda_n) = 0 \quad n = 1, 2, \ldots \tag{9}$$

The analytical step response shown above will be used to validate models in the time-domain. Note that $\Delta C_s(s)$ in Eq. (6) is the

Laplace transform of $\Delta c_s(t)$. $\Delta c_{s,\text{step}}(t)$ in Eq. (7) is the step response of surface concentration relative to the average concentration in the time-domain.

A general state space model is typically written as follows:

$$\begin{aligned} \dot{x} &= Ax + Bu \\ y &= Cx + Du \end{aligned} \tag{10}$$

x is the state vector; y is the output vector; u is the input vector; A, B, C, D are constant coefficient matrices of proper sizes. Since Eq. (10) is linear with constant coefficients, the system is an LTI system. For the state space model used to simulate the solid-phase diffusion problem, x has no physical meaning; y is a scalar representing surface concentration relative to the average concentration, $\Delta c_s(t)$; u is a scalar representing the transient wall flux, $j(t)$. Matrix D becomes zero for the diffusion problem since a step change in $j(t)$ does not cause a step increase in surface concentration. Taking the Laplace transform of Eq. (10) gives the transfer function of the state space model,

$$Y(s)/U(s) = C(sI - A)^{-1}B \tag{11}$$

Its equivalent rational form is the following:

$$H_{ca}(\vec{c}, \vec{a}, s) = Y(s)/U(s) = \sum_{i=1}^{N} \frac{c_i}{s - a_i} \tag{12}$$

where $\vec{c} = [c_1, \ldots, c_N]$, $\vec{a} = [a_1, \ldots, a_N]$ are the residuals and poles of the transfer function, and N is the order of the state space model.

From the final-value theorem, we could put a constraint on Eq. (12), namely $\lim_{s\to 0}$ Eq.(12) $= \lim_{s\to 0}$ Eq.(6) (see Appendix A), to enforce that Eq. (12) has no steady state error,

$$\sum_{i=1}^{N} -\frac{c_i}{a_i} = -\frac{R}{5D} \tag{13}$$

An equivalent form of Eq. (12) with the constraint of Eq. (13) is the following,

$$Y(s)/U(s) = Z + \sum_{i=1}^{N} \frac{\hat{c}_i s}{s - \hat{a}_i} \tag{14}$$

subject to,

$$Z + \sum_{i=1}^{N} \hat{c}_i = 0 \tag{15}$$

and

$$Z = -\frac{R}{5D} \tag{16}$$

where $\hat{c}_i$ and $\hat{a}_i$ are new model constants similar to c_i and a_i that need to be identified if the constrained version of the transfer function of Eq. (14) is used. An advantage of Eq. (14) is that it gives an explicit expression for the steady state value, namely Z. The constraint of Eq. (15) is to satisfy initial value of zero under unit step input. This is derived in a similar fashion as shown in Appendix A using the initial-value theorem.

Eq. (12) without the constraint of Eq. (13) is used in this paper mainly because the VF method used in this paper requires the form of Eq. (12). However, the method does allow one to minimize the steady state error by using a different approach rather than using the constraint of Eq. (13). More specifically, when a weight function with a heavy weight on frequency of zero is used, the steady state error will be minimized. Note that the VF method without a weight function already gives very negligible steady state error. So, a weight function is hardly needed to minimize the steady state error using the VF method. Weight functions will be discussed in details in Section 3.

In using the state space model to model the diffusion process, the goal is to identify Eq. (12) with the system transfer function, Eq. (6), for $s = j\omega$. If we denote the sampled system transfer function of Eq. (6) to be $H(s_i = j\omega_i)$ $i = 1,\ldots,M$, with $M > N$, the problem amounts to generating a state space model of Eq. (10) such that the error

$$E(\vec{c}, \vec{a}, s) = H_{ca}(\vec{c}, \vec{a}, s) - H(s) \tag{17}$$

evaluated at the discrete frequency points, is minimized in some appropriate norm. A least-squares solution can be obtained by minimizing

$$f(\vec{c}, \vec{a}) = \sqrt{\sum_{i=1}^{M} \|H_{ca}(\vec{c}, \vec{a}, s_i) - H(s_i)\|_2^2} \tag{18}$$

Minimization of Eq. (18) is a non-linear problem. The VF method is used in this paper, which is a robust iterative method to solve the minimization problem. A brief explanation of the VF method applied to the diffusion problem is shown in Appendix B. Details about the VF method can be found in Ref. [10].

2.1. A spherical particle test

Property values used in the test case, defined in Table 1, are typical of solid state diffusion in electrochemical cells. The characteristic time $t \approx (R^2/D) = 5000$ s indicates that it can take over an hour for solid-phase concentration gradients to relax. High power HEV batteries, however, may become solid state transport limited in as little as 5 s [18]. To capture these disparate timescales, solution up to 10 Hz is sampled for model identification. Such a frequency is referred to as cut-off frequency for model identification in this paper.

Fig. 1 compares the frequency response of the state space models with the analytical frequency response, Eq. (6). The 5th order state space model gives better accuracy than the 3rd order state space model. Results in Fig. 1 do not appear very accurate especially for high frequency components. This is because the VF method by default uses the 2-norm to minimize the error in the frequency-domain without a weight function, as shown in Eq. (18). Since high frequency components have much less magnitudes, as shown in Fig. 1, VF sacrifices their accuracy. If one checks the error quantitatively, the VF error in 2-norm is actually only 3.2% and 0.67% for the 3rd order and 5th order model, respectively. The large *apparent* error in Fig. 1 is due to logarithmic scale used in the plot. Fig. 2 compares the solution in time-domain under unit step input. The "analytical" solution in the time-domain is approximated by taking the first 5000 terms in Eq. (7). Both models give excellent results compared with the analytical solution as shown in Fig. 2. The small difference between the 3rd order state space model and the analytical solution is only visible in the logarithmic time scale plot, Fig. 2b. Most signals, including the unit step, have large portion of low frequency components and small portion of high

Table 1
Spherical particle model parameters.

Parameter value	Value
Diffusion coefficient, D ($m^2\ s^{-1}$)	2.0×10^{-16}
Particle radius, R (m)	1.0×10^{-6}

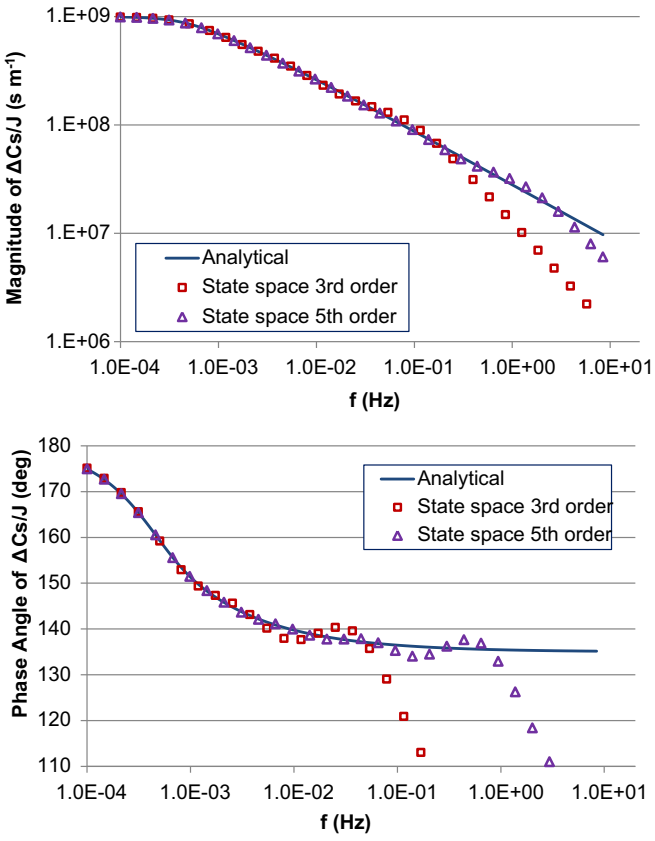

Fig. 1. Frequency responses from the analytical solution of Eq. (6) compared with those from the 3rd order and the 5th order space models.

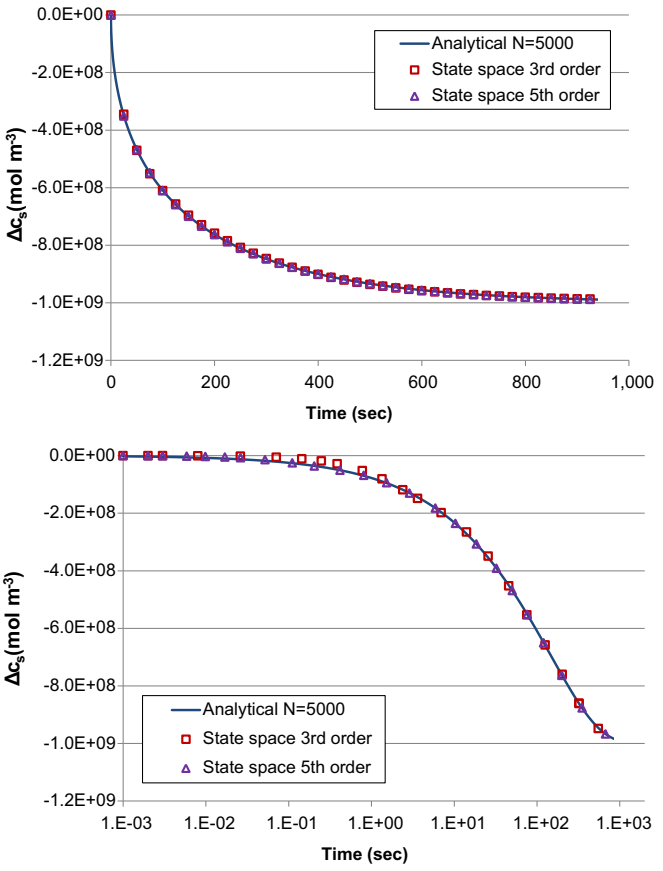

Fig. 2. Unit step responses from the analytical solution and two state space models. a) Regular time scale. b) Log time scale.

frequency components. So, the 2-norm used by VF without a weight function makes time-domain results accurate for most signals. This explains very accurate time-domain results by just a 3rd order state space model. Also note that results in Fig. 2 show negligible steady state error without using any weight function.

If one has a signal with only high frequency components, then even the 5th order model will not give accurate results. To demonstrate this, a 10th order model is generated, which gives much better accuracy in high frequency band compared with the 5th order model. The frequency response of the 10th model is shown in Fig. 3. A pure sinusoidal signal of 1 Hz is sent to the 5th order state space model and the 10th order state space model. Their responses are compared in Fig. 4. It is clear the 5th order state space model deviates from the solution of the 10th order state space model. But practically, when the reduced model is integrated into the physics-based cell models, the reduced model is unlikely to experience such a high single frequency signal. Even if such a single frequency signal is used at the boundary of the physics-based model, the particle wall flux will not have such a single frequency since the physics-based model is non-linear. However, if significant high frequency components are present, VF can generate higher order models to give accurate results. In such a case, the full model also needs more grid resolution for accuracy. So, it is still beneficial to use the reduced model.

3. Vector fitting with weight functions

A weight function can be added when performing VF to give more weight to certain frequency band. Eq. (18) with a weight function becomes:

$$f(\vec{c}, \vec{a}) = \sqrt{\sum_{i=1}^{M} w(s_i) \cdot \|H_{ca}(\vec{c}, \vec{a}, s_i) - H(s_i)\|_2^2} \tag{19}$$

A weight function giving high frequency components more weight is used to demonstrate the effect of the weight function on the frequency response. Since the magnitude of the system response decreases exponentially, the weight function used has an exponential form of 1.07^i to bring all frequency components to approximately the same magnitude. The number 1.07 was chosen by trial and error to give the results shown in Fig. 5. It is clear from Fig. 5 that the frequency response from the model with a weight function favoring high frequencies *appears* to be more accurate. However, the time-domain performance of the model under a unit step input is worse as shown in Fig. 6. This is because while favoring high frequency its low frequency accuracy is compromised. A unit step signal, like many other signals, has more components in low frequency than in high frequency. Therefore, the time-domain performance of a model favoring high frequencies is not as accurate under a unit step input. Note that the weighted 5th order state space model has a noticeable steady state error. Using the final-value theorem, the same conclusion can be drawn from its frequency response as frequency approaches zero. A way to improve the steady state solution is to put more weight on very low frequency components. But if we put weight on both low and high frequencies, the midfrequency components will have poor performance. After all, we only have 10 degrees of freedom at our disposal to optimize Eq. (19) using a 5th order state space model.

Ultimately the state space model will be integrated into the physics-based cell models and these models are highly non-linear

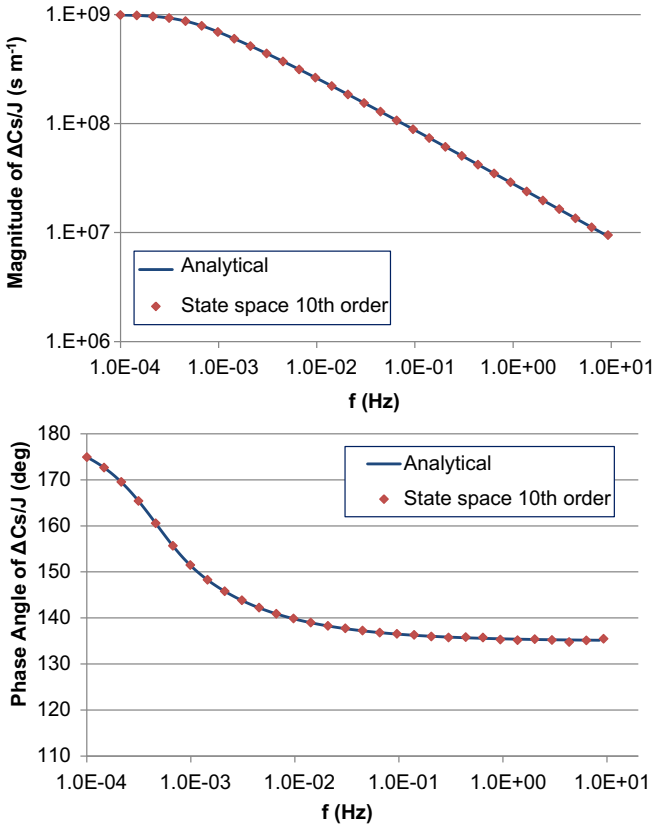

Fig. 3. Frequency responses from the analytical solution of Eq. (6) compared with those from the 10th order state space model.

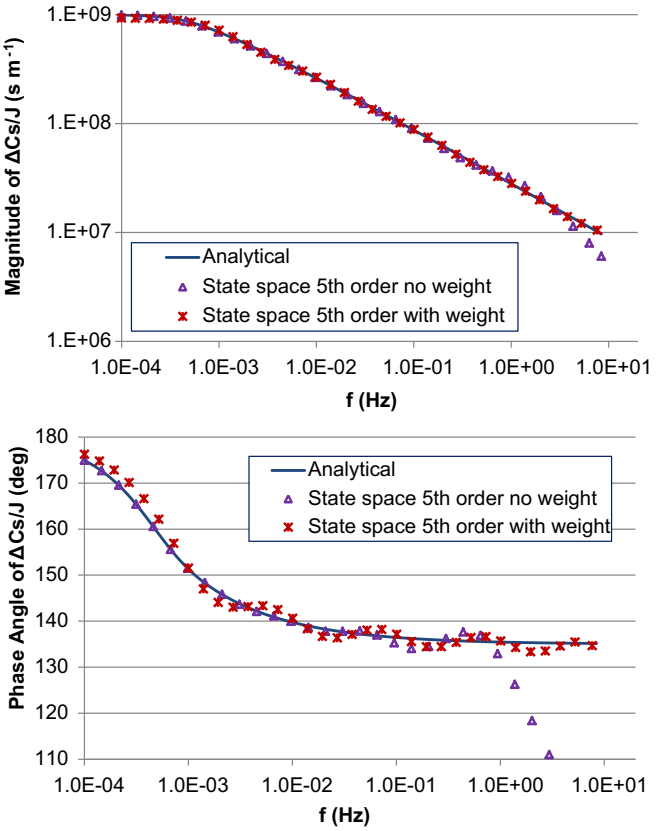

Fig. 5. Frequency responses from the analytical solution of Eq. (6) compared with those from two 5th order state space models with and without weight function.

overall. As shown above, adding weight function to make frequency response *look* more accurate might not always be desirable. To make sure that the state space model gives accurate results for enough frequency range, one could run the full physics-based model using signals containing reasonably high frequency components and record the $j(t)$ at the particle surface. An FFT of $j(t)$ tells what frequency contents are present at the particle surface. Based on that information, a judicious decision can be made as for what cut-off frequency to be used and what weight function, if any, to be used when generating the state space model. The benefit of using the VF method in identifying state space models is that it can accommodate all these requests easily and robustly. More details on how to integrate the reduced order model into the physics-based cell models are shown in Ref. [9].

4. Model development when analytical transfer functions are not available

We showed how to create state space models for particle diffusion problems when the transfer function is known. For spherical particles, the transfer function of the system has an analytical form of Eq. (6). For non-spherical particles, we need to approximate system transfer functions numerically before VF can be used to identify state space models. In this section, we demonstrate how to obtain transfer functions accurately using numerical

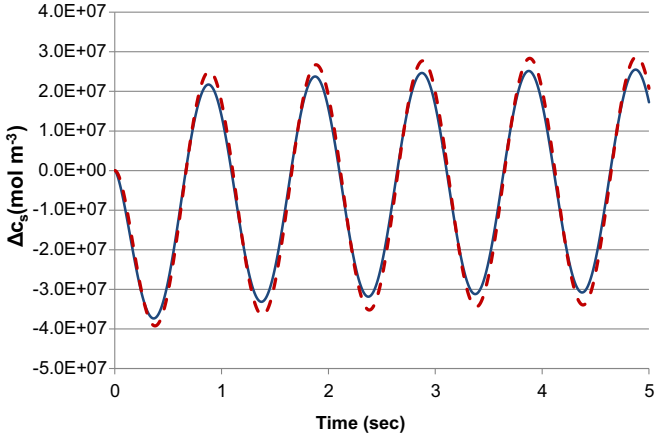

Fig. 4. Responses of 5th order and 10th order state space models under 1 Hz sinusoidal signal. Solid line is for 10th order; dash line is for 5th order.

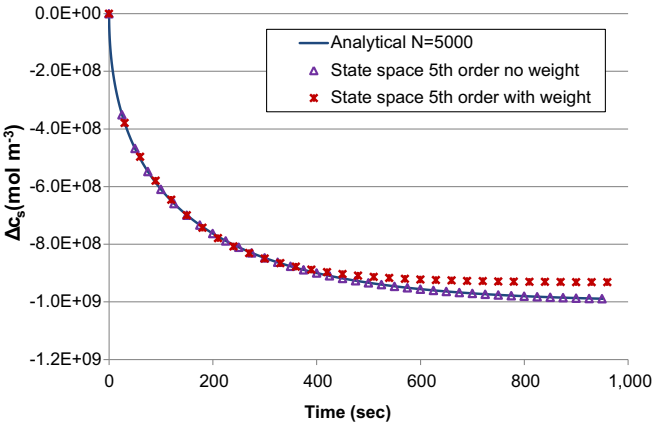

Fig. 6. Step responses from the analytical solution of Eq. (6) compared with those from two 5th state space models with and without weight function.

methods. Spherical particles will be used since analytical solution exists to help validate the methodology. So, the analytical transfer function is not used in the model identification process. The analytical transfer function is only used to validate results.

4.1. Step response method to obtain frequency response

One way to calculate the system transfer function is to calculate the Laplace transform of the impulse response of the system. As a matter of fact, Laplace transform of the impulse response of a system is one way to define transfer function. But since it is difficult to obtain the impulse response accurately, we obtain the step response first and then calculate the time derivative of the step response to obtain the impulse response. Such a procedure can be used for non-spherical particles since step responses can be obtained by numerical methods regardless of the shape of the particle.

The response of a spherical particle under a unit step input of 1 mol m^{-2} s^{-1} is Eq. (7). The time derivative of the unit step response becomes the unit impulse response, which is the following,

$$\frac{d[\Delta c_s(t)]}{dt} = \sum_{n=1}^{\infty}\left[-\frac{2}{R}\exp\left(-\lambda_n^2\frac{D}{R^2}t\right)\right] \quad (t>0) \tag{20}$$

where λ_n is defined in Eq. (9). If the unit step response is obtained by numerical methods, the unit impulse response can be calculated by taking numerical derivative.

Fourier transfer of Eq. (20) becomes the frequency response of the system, namely Eq. (6) with $s = j\omega$. However, to make the process general, we are not assuming we could obtain analytical expression for the impulse response. So, sampled version of Eq. (20) will be used. FFT of the sampled impulse response, after proper scaling, becomes the numerically calculated frequency response at discrete frequency values. And frequency response at discrete frequency values is what we need to perform VF to identify the state space model. Fig. 7 shows three numerically obtained frequency responses by using sampling frequencies of 5 Hz, 50 Hz, and 100 Hz, respectively. As sampling frequency becomes higher, the numerically calculated frequency response becomes more accurate. Note that we obtained the sampled impulse response from the analytical solution of Eq. (20), approximated by taking the first 5000 terms. So, there is a minimum amount of numerical error in this process. When an impulse response is calculated numerically from a step response, which in turn is from numerical methods, it is difficult to obtain accurate results for high frequencies. Therefore, the step response method can only give accurate results to relatively low frequencies.

4.2. Complex exponential method to obtain frequency response

The step response method can be used to obtain accurate frequency response for low frequencies. But it could involve large numerical error for high frequencies. The complex exponential method proposed in this section can be used to obtain accurate frequency response at discrete frequency values for high frequencies. Such a method is widely used in high frequency electromagnetics to calculate the solution in the frequency-domain [19]. The complex exponential method relies on the fact when a complex exponential function $\exp(j\omega_0 t)$ is used as an input to a linear system, the complex amplitude of the output equals the frequency response of the system at ω_0. This can be derived from the fact that the Fourier transfer of the complex exponential is $2\pi\delta(\omega-\omega_0)$, where δ is a Dirac delta function. This feature allows us to calculate the frequency response at ω_0 by calculating the complex amplitude of the output for an input of $\exp(j\omega_0 t)$.

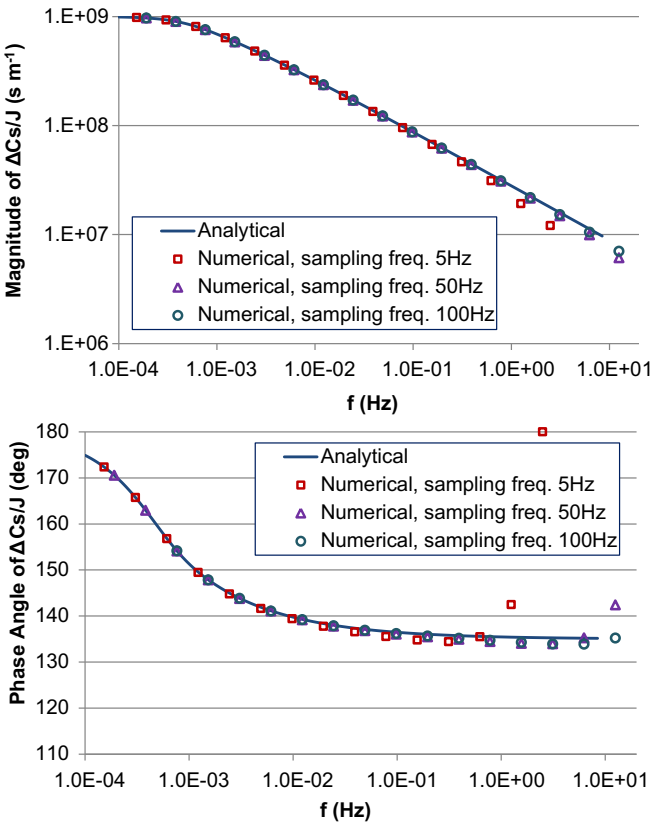

Fig. 7. Frequency responses from the analytical solution of Eq. (6) compared with those from the step response method.

Let $j(t) = \exp(j\omega t)$ and $c(r,t) = C(r)\exp(j\omega t)$, where C is a complex concentration distribution. Substituting the above into Eq. (1) and separating real and complex parts gives the following governing equation for complex concentration distribution, C,

$$\begin{cases} -\omega C_i = D\dfrac{1}{r^2}\dfrac{\partial}{\partial r}\left(r^2\dfrac{\partial C_r}{\partial r}\right) \\ \omega C_r = D\dfrac{1}{r^2}\dfrac{\partial}{\partial r}\left(r^2\dfrac{\partial C_i}{\partial r}\right) \\ \left.\dfrac{\partial C_r}{\partial r}\right|_{r=0} = \left.\dfrac{\partial C_i}{\partial r}\right|_{r=0} = 0 \\ \left.-D\dfrac{\partial C_r}{\partial r}\right|_{r=R} = 1 \\ \left.\dfrac{\partial C_i}{\partial r}\right|_{r=R} = 0 \end{cases} \tag{21}$$

where C_r and C_i are the real and imaginary part of C. Note that Eq. (21) has no time dependency. The frequency response we need is for the surface concentration relative to average concentration. The complex average concentration from complex exponential input can be shown to be $3j/(R\omega)$. After solving Eq. (21) for C, evaluating C at the surface minus complex average concentration gives the desired frequency response at frequency of ω. Solving Eq. (21) multiple times for discrete values of ω gives the frequency response at those discrete frequency values.

Eq. (21) is a pair of coupled Poisson equations, which can be solved easily. FLUENT, a computational fluid dynamics (CFD) code by ANSYS Inc. [20], is used to solve Eq. (21) in this paper. Fig. 8 shows the frequency response at discrete frequency values calculated using the complex exponential method compared with the analytical frequency

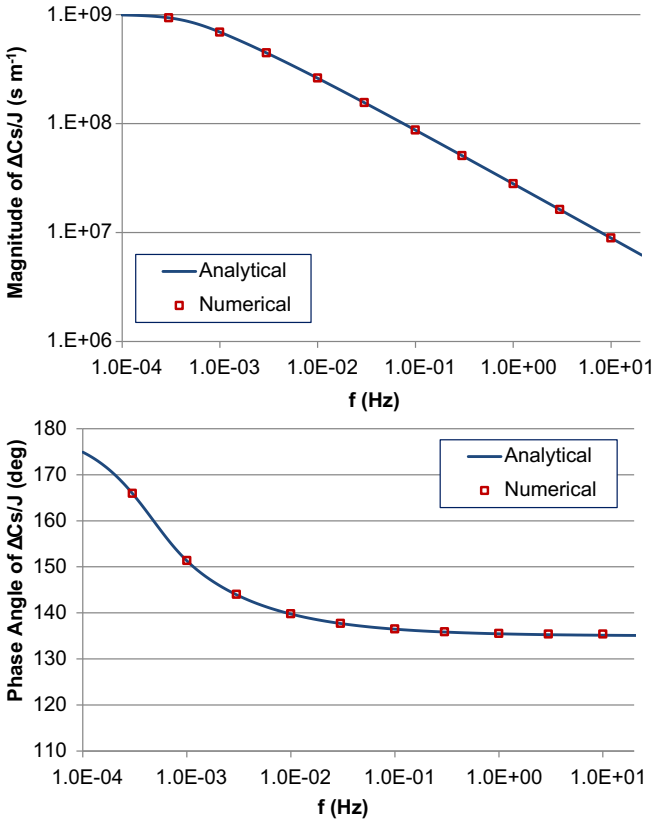

Fig. 8. Frequency responses from the analytical solution of Eq. (6) compared with those from the complex exponential method.

response. Fig. 8 shows that this method gives highly accurate results for frequency as high as 10 Hz, while the step response method, when sampling even at 100 Hz, is less accurate at high frequencies as shown in Fig. 7. At low frequencies, both methods give excellent results. Note that the complex exponential method solves a steady state problem rather than a transient problem. Therefore, in using the complex exponential method, we do not have to concern about time. We also do not need to worry about sampling in using the complex exponential method. But in using the complex exponential method, multiple steady state simulations are needed as opposed to solving just one transient simulation in the step response method. When using the complex exponential method, we noticed that for very low frequencies it is hard to converge Eq. (21). So, when accurate high frequency solution is not needed, the step response method is sufficient. Otherwise, the complex exponential method could be used to calculate the frequency response at high frequencies.

An interesting observation was obtained when solving Eq. (21). Fig. 9 shows the contour of magnitude of complex concentration at a frequency of 0.1 Hz. Note that even at such a seemingly low frequency of 0.1 Hz concentration is highly concentrated near the surface. This suggests that the curvature of the sphere has negligible impact on the solution at this frequency. To verify this, we utilize the analytical solution that exists when the radius is infinity, namely a wall instead of a sphere. The analytical frequency response can be shown to be the following (see Appendix C),

$$H(j\omega) = \frac{-1+j}{\sqrt{4\pi fD}} \tag{22}$$

The above frequency response is compared with that of a spherical particle with a radius of 1 μm in Fig. 10. It is clear for Fig. 10 that the behavior of the spherical particle starts to differ from a wall at

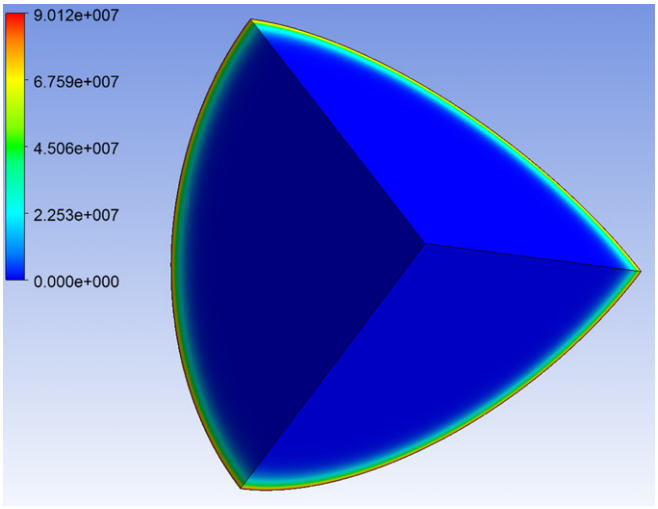

Fig. 9. Contour of magnitude of complex concentration C (mol m^{-3}) at a frequency of 0.1 Hz.

a frequency of approximately 0.1 Hz. From this result, it is clear that 0.1 Hz for this particle is really high.

This rather interesting observation can be further explained by penetration length, defined by the location where the magnitude has decreased to 1% of the wall value. For the wall, the penetration length has the following analytical expression (see Appendix C),

$$\delta \approx 4.6\sqrt{\frac{D}{\pi \cdot f}} \tag{23}$$

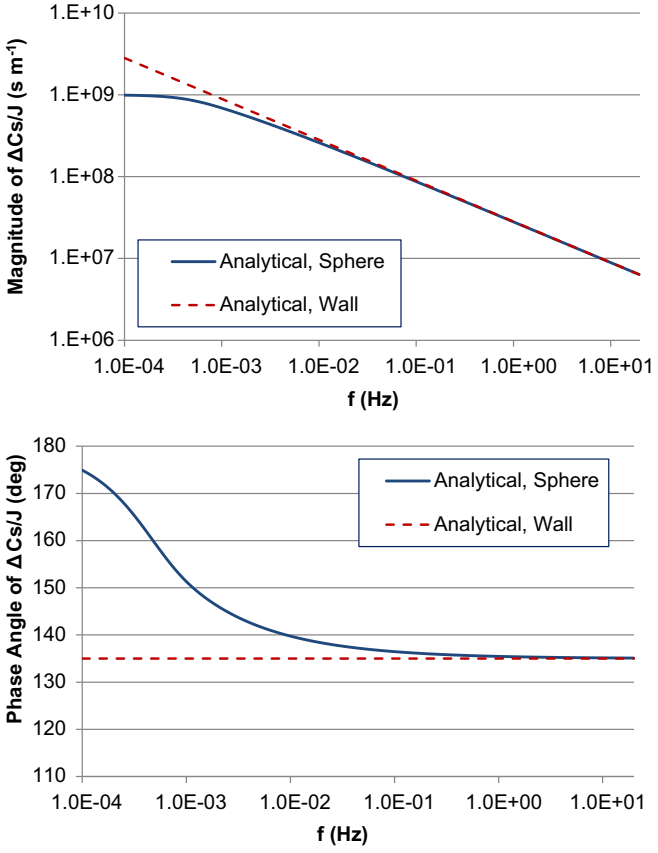

Fig. 10. Analytical frequency responses of Eq. (6) for a sphere compared with those from Eq. (C.9) for a wall.

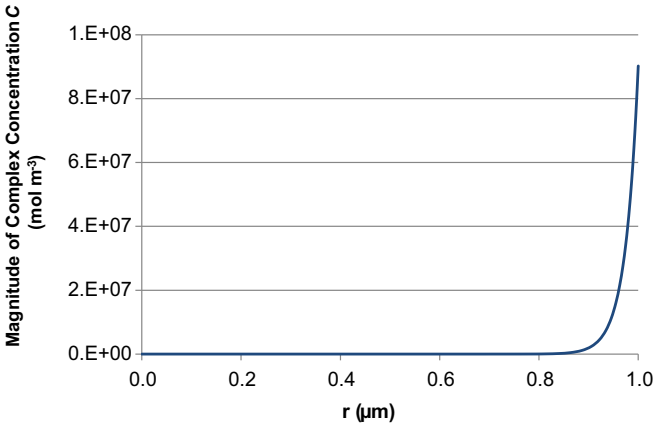

Fig. 11. Magnitude of complex concentration C as a function of r for the spherical particle at a frequency of 0.1 Hz under wall flux with unit magnitude.

At a frequency of 0.1 Hz, the penetration length is approximately 0.116 μm. For the spherical particle, the penetration length can be found by plotting the concentration as a function of r, which is shown in Fig. 11. From the plot, the penetration length can be found to be 0.121 μm. This is within 5% of the value for the wall confirming that the particle with a radius of 1 μm behaves like a wall at a frequency of 0.1 Hz! Such information helps designers to determine what the optimum particle size is for the diffusion process. If the wall flux $j(t)$ has a large portion of frequency components close to 0.1 Hz, it is clearly advantageous to use smaller particles to increase the particle specific interfacial area to enhance diffusion. Note that the above conclusion is based on the diffusion coefficient used in Table 1.

Once the reduced order model is identified for the diffusion process, the model can be integrated into the physics-based Newman electrochemistry pseudo-2D model. Such an integration progress and its validation against solving the diffusion equations numerically are discussed in Ref. [9].

5. Conclusion

A model order reduction method is developed and applied to the solid-phase diffusion problem used in physics-based lithium ion cell models. Model identification is performed in the frequency-domain using the vector fitting method. The method allows the user to control the order of the model, the frequency band for model identification, and optionally a weight function to give certain frequency band more weight. The model shows excellent accuracy with a 5th order model. The 3rd order model shows a small deviation from analytical solution when logarithmic time scale is used. Since the reduced model solves only a few equations, it runs much faster than the model for the full diffusion equation.

The method can be used for non-spherical particles. When doing so, system responses need to be calculated numerically. Two methods are demonstrated. The step response method is easy to use and gives accurate results for low frequencies. The complex exponential method could be used to obtain highly accurate results at high frequencies but it is hard to converge at low frequencies.

List of symbols

c	concentration, mol m^{-3}
c_{ave}	average particle concentration, mol m^{-3}
c_s	surface concentration, mol m^{-3}
C	complex concentration
C_{ave}	Laplace transform of average concentration
C_s	Laplace transform of surface concentration
D	diffusivity of lithium in the solid particles, m^2 s^{-1}
R	radius of the spherical particle, m
j	wall flux of lithium ions, mol m^{-2} s^{-1}
J	Laplace transform of wall flux of lithium ions
w	weight function for vector fitting
Δc_s	surface concentration relative to average concentration, mol m^{-3}
$\Delta c_{s,step}$	step response of surface concentration relative to average concentration, mol m^{-3}
ΔC_s	Laplace transform of surface concentration relative to average concentration, $C_s - C_{ave}$
δ	penetration length, m
λ_n	eigenvalues of the diffusion problem

Abbreviations

FFT	Fast Fourier Transform
LTI	Linear and Time-Invariant
VF	Vector Fitting

Appendix A. A constraint on numerical transfer function to enforce zero steady state error under step input from the final-value theorem

The final-value theorem says the following. If $\Delta C_s(s)$ is the Laplace transform of $\Delta c_s(t)$, then

$$\lim_{t\to\infty} \Delta c_s(t) = \lim_{s\to 0} s\Delta C_s(s) \tag{A.1}$$

From Eq. (6), we obtain $\Delta C_s(s) = H(s)J(s)$. If $J(s)$ is the Laplace transform of a unit step function, then,

$$\Delta C_s(s) = \frac{H(s)}{s} \tag{A.2}$$

Substituting Eqns. (A.2) into (A.1) gives the following,

$$\lim_{t\to\infty} \Delta c_s(t) = \lim_{s\to 0} H(s) \tag{A.3}$$

Therefore, if we want to enforce zero steady state error under step input, we need the following constraint on the numerical transfer function, namely,

$$\lim_{s\to 0} \sum_{i=1}^{N} \frac{c_i}{s-a_i} = \lim_{s\to 0} H(s) \tag{A.4}$$

Appendix B. Model identification process for the diffusion problem using vector fitting

In using the VF method for state space model identification, the transfer function of the state space model is identified with the transfer function of the diffusion problem. The transfer function of the state space model in Eq. (10) can be shown as following:

$$f(s) = \sum_{i=1}^{N} \frac{c_i}{s-a_i} \tag{B.1}$$

The fitting process can be viewed as using rational basis functions $1/(s-a_i)$ for curve-fitting to find c_i. If a_i were known, this would become a linear least-squares problem to determine c_i. Since a_i are not known, an iterative scheme is needed to update a_i at each iteration. Once the poles and residuals are obtained, it is a simple realization problem to obtain the corresponding state space model of Eq. (10). Such a fitting approach in the frequency-domain is

generally referred to as rational fitting. VF is a robust algorithm of rational fitting first proposed in Ref. [10].

The steps to identify the state space model using VF are summarized as follows:

Step 1. Obtain the transfer function of the diffusion problem numerically or analytically.
Step 2. Perform vector fitting to obtain the poles and residuals of the transfer function of the state space model.
Step 3. Construct the state space model from the known transfer function, which is obtained from Step 2.

Appendix C. Analytical solution for a wall diffusion problem under complex exponential flux boundary condition

The governing equations for the diffusion problem in an infinite wall are

$$\frac{\partial c}{\partial t} = D\frac{\partial^2 c}{\partial z^2} \tag{C.1}$$

$$c(z, t = 0) = 0 \tag{C.2}$$

$$-D\frac{\partial c}{\partial z}\bigg|_{z=0} = -j(t) \tag{C.3}$$

where z is the coordinate going into the wall. The extra minus sign in Eq. (C.3) compared with Eq. (4) is due to the convention that positive $j(t)$ points outside of the domain.

Let $j(t) = \exp(j\omega t)$ and $c(z, t) = C(z)\exp(j\omega t)$, where C is complex concentration distribution. Substituting the above into Eq. (C.1) and Eq. (C.3) gives the following,

$$j\frac{\omega}{D}C = \frac{\partial^2 C}{\partial z^2} \tag{C.4}$$

$$-D\frac{\partial C}{\partial z}\bigg|_{z=0} = -1 \tag{C.5}$$

A trial solution of the form $C = \exp(jkz)$ leads to the condition:

$$k^2 = -\frac{\omega}{D}j \tag{C.6}$$

This leads to a solution of C

$$C = c_1 \exp\left[-(1+j)\sqrt{\frac{\omega}{2D}}z\right] \tag{C.7}$$

The second exponential term drops since it goes to infinity as z goes to infinity. Boundary condition Eq. (C.5) can be used to determine the constant in Eq. (C.7). The final expression for C is the following

$$C = \frac{-1+j}{\sqrt{2\omega D}} \exp\left[-(1+j)\sqrt{\frac{\omega}{2D}}z\right] \tag{C.8}$$

Evaluating C at $z = 0$ gives

$$C(0) = \frac{-1+j}{\sqrt{4\pi f D}} \tag{C.9}$$

Eq. (C.9) is the frequency response of surface concentration. To obtain the frequency response of the surface concentration relative to the average concentration, we need to subtract the average value. But since the wall has infinite size, the average value is zero.

To obtain the penetration length, defined by the location where the magnitude has decreased to 1% of the wall value, we let the exponential term in Eq. (C.8) delays to 0.01,

$$\exp\left(-\sqrt{\frac{\omega}{2D}}\delta\right) = 0.01 \tag{C.10}$$

This leads to

$$\delta \approx 4.6\sqrt{\frac{D}{\pi \cdot f}} \tag{C.11}$$

References

[1] M. Doyle, T.F. Fuller, J. Newman, J. Electrochem. Soc. 140 (6) (1993) 1526–1533.
[2] T.F. Fuller, M. Doyle, J. Newman, J. Electrochem. Soc. 141 (1) (1994) 1–10.
[3] M. Doyle, J. Newman, J. of Electrochem. Soc. 143 (6) (1996) 1890–1903.
[4] C.Y. Wang, W.B. Gu, B.Y. Liaw, J. Electrochem. Soc. 145 (10) (1998) 3407–3417.
[5] V.R. Subramanian, D. Tapriyal, R.E. White, Electrochem. Solid-State Lett. 7 (9) (2004) A259–A263.
[6] M. Guo, R.E. White, J. Power Sources 198 (2012) 322–328.
[7] K.A. Smith, C.D. Rahn, C.Y. Wang, J. Dyn. Syst. Meas. Control 130 (011012) (2008) 1–8.
[8] J.L. Lee, A. Chemistruck, G.L. Plett, J. Power Sources 206 (2012) 367–377.
[9] X. Hu, S. Stanton, L. Cai, R.E. White, J. Power Sources 214 (2012) 40–50.
[10] B. Gustavsen, A. Semlyen, IEEE Trans. Power Del. 14 (3) (1999) 1052–1061.
[11] A. Morched, B. Gustavsen, M. Tartibi, IEEE Trans. Power Del. 14 (3) (1999) 1032–1038.
[12] B. Gustavsen, IEEE Trans. Power Del. 19 (1) (2004) 414–422.
[13] E.P. Li, E.X. Liu, L.W. Li, M.S. Leong, IEEE Trans. Adv. Packag. 27 (1) (2004) 213–223.
[14] G. Antonini, IEEE Trans. Electromagn. Compat. 45 (3) (2003) 502–512.
[15] X. Hu, S. Lin, S. Stanton, W. Lian, IEEE Trans. Ind. Appl. 47 (4) (2011) 1692–1699.
[16] X. Hu, L. Chaudhari, S. Lin, S. Stanton, S. Asgari, W. Lian, in: IEEE ITEC Conf. in Dearborn, 2012, IT-0065.
[17] T. Jacobsen, K. West, Electrochim. Acta 40 (1995) 255–262.
[18] K. Smith, C.Y. Wang, J. Power Sources 161 (2006) 628–639.
[19] S. Ramo, J.R. Whinnery, T. Van Duzer, Fields and Waves in Communication Electronics, third ed. John Wiley & Sons, 1994.
[20] ANSYS, online: http://www.ansys.com/ (accessed 28.06.12).